Int J Clin Exp Med 2018;11(3):1615-1631
www.ijcem.com /ISSN:1940-5901/IJCEM0057902

Original Article

Apigenin inhibits proliferation of human chondrosarcoma cells via cell cycle arrest and mitochondrial apoptosis induced by ROS generation-an *in vitro* and *in vivo* study

Xiao-Bo Yan[1], Tao Xie[2], Sheng-Dong Wang[1], Zhan Wang[1], Heng-Yuan Li[1], Zhao-Ming Ye[1]

[1]*Department of Orthopedics, Second Affiliated Hospital, School of Medicine, Zhejiang University, Hangzhou, China;* [2]*Department of Orthopedics, Hangzhou First People's Hospital, Nanjing Medical University, Hangzhou, China*

Received March 24, 2017; Accepted November 20, 2017; Epub March 15, 2018; Published March 30, 2018

Abstract: Objective: Classical chondrosarcoma has poor sensitivity to chemotherapy and radiotherapy, and surgical resection is the only effective treatment. Therefore, development of a novel adjuvant therapy is required. In vitro and in vivo studies have found that apigenin, a type of flavonoid, has anti-tumor activity in various malignancies. The effects of apigenin on human chondrosarcoma and the mechanisms underlying these effects remain unknown. Methods: Here we used different concentration of Apigenin to treat chondrosarcoma cells. Cell viability, Clone formation, Cell cycle, typical apoptotic morphological changes were identified by optical microscopy, Hoechst staining, and transmission electron microscopy. The early and total apoptotic rate was estimated by flow cytometry. Results: We found here apigenin inhibits chondrosarcoma cell proliferation by inducing G2/M phase arrest and inhibiting colony formation. Apigenin treatment induced mitochondrial apoptosis of chondrosarcoma cells by regulating the expression of the Bcl-2 family and activating the Caspase cascade. Exposure to apigenin induced marked ROS generation, reduced the mitochondrial membrane potential, and created an imbalance in intracellular calcium concentration in sw1353 cells. Conclusion: We consider ROS generation to be the major mechanism of apoptosis induction by apigenin. *In vivo*, apigenin suppressed tumor growth in a mouse xenograft model. Taken together, these results suggest that apigenin exhibits anti-tumor efficacy against chondrosarcoma *in vitro* and *in vivo*. Apigenin inhibits proliferation and induces mitochondrial apoptosis via ROS generation in human chondrosarcoma cells. Thus, apigenin is a promising novel adjuvant agent for chondrosarcoma therapy.

Keywords: Chondrosarcoma, apigenin, cell cycle arrest, ROS, mitochondrial apoptosis

Introduction

Chondrosarcoma, a malignant cartilage tumor, is one of the most common bone sarcomas. It is the third most common primary bone tumor, following myeloma and osteosarcoma [1]. The annual incidence of chondrosarcoma is 9%, half that of osteosarcoma [2]. One characteristic of chondrosarcoma is its wide range of onset age, as adults aged 25-60 years are at risk of developing this disease. Another is its extensive pathogenetic localisation. Chondrosarcoma may occur in any part of the skeleton or soft tissue, but it is more common in the lower body, including the pelvis, vertebra, proximal humerus, and femur [3]. Chondrosarcoma is relatively insensitive to chemotherapy and radiotherapy-surgical resection is the only effective treatment [4]. When a tumor develops at a site that cannot be resected completely, partial recurrence is possible due to the lack of an effective adjuvant treatment that kills residual tumor cells. Cartilage is a relatively avascular tissue; thus, cancer cells are more likely to become implanted, leading to recurrence [4]. Most recurrent chondrosarcomas have a higher histological grade and thus a poorer prognosis than the original lesion [5]. Therefore, the development of novel adjuvant therapies for the management of chondrosarcoma is urgently required.

Apigenin (4',5,7-trihydroxyflavone), a flavonoid that is abundant in the human diet, is contained in such food as fruits and vegetables. Apigenin

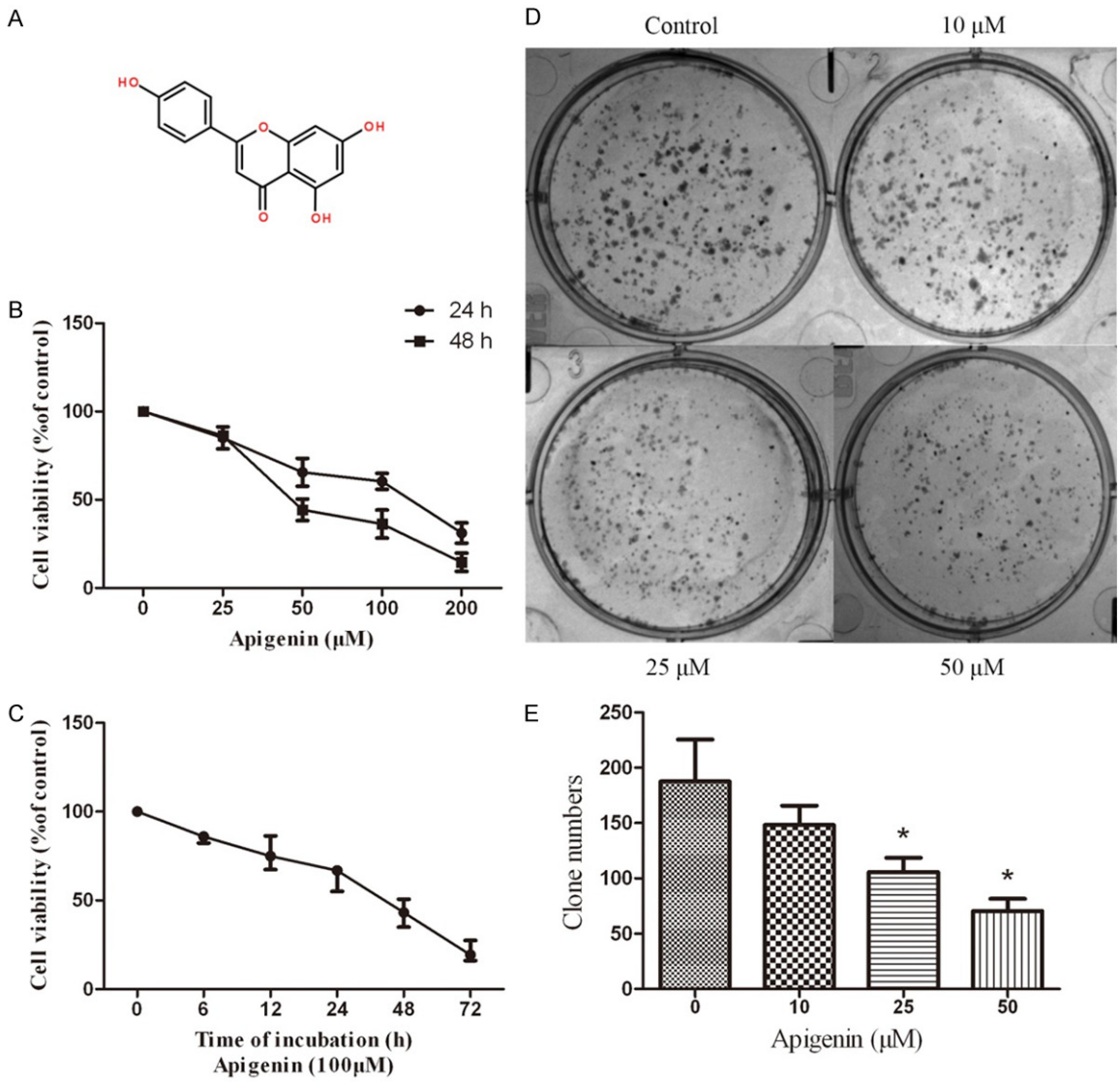

Figure 1. Apigenin inhibited the growth of human chondrosarcoma cells in a dose- and time-dependent manner. A. The chemical structure of apigenin. B. The anti-proliferative effect of apigenin on sw1353 chondrosarcoma cells was determined by MTS assay. Cells were treated with various concentrations of apigenin for 24 or 48 h. The control group was treated with 0.1% DMSO. Data are the means of five replicates, each of which was performed in triplicate. C. Cell viability after treatment with 100 μM apigenin for 72 h. D. Colony formation by sw1353 cells at 14 days subjected to the control or apigenin treatment. E. sw1353 colonies were enumerated. Data are means ± S.D. of triplicate independent experiments. $^{*}P < 0.05$ compared with the control group.

has received attention recently because of its chemopreventive effects and anti-inflammatory and anti-tumor activities. Shukla demonstrated that apigenin inhibited prostate cancer proliferation by inducing cell cycle arrest [6]. Furthermore, apigenin has been reported to induce apoptosis in various malignancies [7, 8]. Chen found that apigenin activated the Bcl-2 pathway in anoxia/reoxygenation-induced myocardium injury [9]. In addition, apigenin has been shown to stimulate excessive reactive oxygen species (ROS) generation, which induces mitochondrial dysfunction and apoptotic cell death [10, 11]. Although these findings suggest anti-tumorigenic activity, the specific mechanism of such action remains unknown. Moreover, whether apigenin suppresses the growth of human chondrosarcoma has not been determined.

Programmed cell death (PCD), type I- apoptosis, the regulated destruction of cells, is a com-

plex process that plays a key role in traditional chemotherapies and novel therapies targeted against various malignant tumors. Apoptosis enables strict control of cell numbers and tissue size and protects against rogue cells that threaten homeostasis [12]. Among the various types of apoptosis, caspase-mediated mitochondrial apoptosis is the most important. Caspases, a set of cysteine proteases that are activated specifically in apoptotic cells, act as central executioners in cell death. It remains to be determined whether and by what underlying mechanism apigenin can induce apoptosis in chondrosarcoma cells.

Reactive oxygen species (ROS), active forms of oxygen, are generated as by-products of cellular metabolism. ROS can promote cell proliferation, differentiation, and survival and play an anti-inflammatory and antibacterial role under oxygen-balanced conditions [1, 2]. Excessive production of ROS causes oxidative damage to cellular lipids, proteins, and DNA, and this then activates intracellular apoptosis, autophagy, and ER-stress signaling pathways to induce cell death [13, 14]. Although cellular oxygen homeostasis imbalance is considered to be involved in tumorigenesis, more pharmaceuticals set ROS as a potential target by inducing oxidative stress causing tumor cell death through apoptosis and autophagy. In this study, we found that apigenin treatment induced excessive ROS generation and then activated the Bcl-2 family proteins, which led to mitochondrial dysfunction and initiated apoptosis.

Although many studies have demonstrated the antineoplastic effects of apigenin in human malignancy, its activity against chondrosarcoma has not been reported. In the present study, we elucidated the inhibitory effect of apigenin on chondrosarcoma cell lines *in vitro* and *in vivo*. We further explored the molecular mechanisms (i.e. induction of G2/M phase arrest, ROS-mediated mitochondrial dysfunction and apoptosis) underlying this process.

Materials and methods

Cells and cell culture

The human chondrosarcoma cell line sw1353 was purchased from the Shanghai Institute of Cell Biology of the Chinese Academy of Sciences (Shanghai, China). Dulbecco's Modified Eagle's Medium (DMEM, high glucose) was supplemented with 10% foetal bovine serum (FBS, Invitrogen, Carlsbad, USA) and 100 μg/ml streptomycin-penicillin. All cells were incubated at 37°C in a 5% CO_2 atmosphere.

Reagents and antibodies

Apigenin (Selleck Chemicals, USA) was dissolved in dimethyl sulfoxide (DMSO) to a concentration of 200 mM and stored at -20°C. The molecular formula of apigenin is $C_{15}H_{10}O_5$, and its molecular weight is 270.24 (**Figure 1A**). Primary antibodies against Cdc2, p-Chk2 (Thr68), Cyclin B1, p-Cdc2, Caspase 3/9, PARP, p21, Bcl-2, p-Bcl-2, Bax, Bid, tBid, Bcl-XL, survivin, and GAPDH were purchased from Cell Signaling Technology (Beverly, MA, USA) and Santa Cruz Biotechnology (SCBT, CAL, USA). A cell cycle PI staining kit and an Annexin V-PE/7-AAD apoptosis detection kit for flow cytometry were purchased from BD Biosciences (Franklin, NJ, USA). A Cell Meter Caspase 3/7 Activity Apoptosis Assay Kit was used in this study (DEVD green fluorescence probe, 511 nm, KeyGEN BioTECH, Nanjing, China). N-Acetyl-L-cysteine (NAC) was purchased from Sigma-Aldrich (St. Louis, MO, USA).

Cell viability assay

Sw1353 cells were seeded in 96-well plates at 3000/well, incubated at 37°C in 5% CO_2, and treated with various concentrations of apigenin for 24 and 48 h. An MTS assay (CellTiter 96AQ, Promega, Beijing, USA) was performed to evaluate cell viability. A fresh mixture of MTS and PMS was added and incubated for 2 to 4 h at 37°C following the provided protocol. An AMR7000 microplate reader was used to measure the absorbance at 490 nm.

Clone formation assay

Sw1353 cells were seeded in six-well plates at 500/well and incubated at 37°C in 5% CO_2 for 3 days. On day 3, when primary clones were observed, we add different concentrations of apigenin (10 μM, 25 μM, 50 μM). Treatment continued for 3 days; apigenin medium was then replaced with non-apigenin-medium, and cells were incubated as described above until visible clones had formed. Cells were fixed with 4% paraformaldehyde for 15 min and stained with 0.1% crystal violet. Clones were observed

under an inverted microscope and enumerated. Images were obtained under enhanced chemiluminescence (ECL) exposure.

Cell cycle analysis

Sw1353 cells were plated in six-well plates at 3 × 10^5 per well and incubated at 37°C in 5% CO_2 with various concentrations of apigenin (50 μM, 100 μM, 150 μM) for 48 h. The cells were harvested by trypsin digestion, washed, resuspended in cold PBS, and fixed in cold 75% ethanol for storage at -20°C overnight. The fixed cells were stained with 40 μg/ml PI for 15 min at room temperature (RT) and then analyzed using flow cytometry and the ModFit LT software.

Cell apoptosis analysis

Sw1353 cells were exposed to various concentrations of apigenin (50 μM, 100 μM, 150 μM) for 48 h in six-well plates at 3 × 10^6 per well. Cells were then harvested, fixed with 4% paraformaldehyde for 20 min, and stained with Hoechst 33258 for 20 min and actin-tracker green for 20 min (Beyotime Biotechnology, Shanghai, China). Typical apoptotic morphological changes were assessed by fluorescence microscopy. The apigenin-treated sw1353 cells were stained using an Annexin V-PE/7-AAD kit (BD Biosciences, San Diego, CA, USA). The cells were resuspended in PBS, centrifuged three times, and then incubated with PE-conjugated annexin V and 7-AAD for 15 min at RT in darkness. Cells were then washed again with PBS and resuspended in 500 μl of 1 buffer supplied in the kit. Samples were analyzed by flow cytometry (FACSCalibur, BD, San Jose, CA, USA) and the CELLQuest software (FACSCalibur).

Measurement of ROS and intracellular calcium concentrations

Reactive oxygen species (ROS) were measured using an ROS assay kit with DCFH-DA (Beyotime). Intracellular calcium concentrations were measured using a Fluo-3am calcium fluorescence probe (Beyotime). In brief, cells were plated at a density of 3 × 10^5/well in six-well plates and exposed to apigenin for 12 h. Then the cells were incubated with DCFH-DA (10 μM) for 30 min at 37°C or Fluo-3am (5 μM) for 20 min at RT. The ROS and intracellular calcium concentrations were determined by fluorescence microscopy and flow cytometry.

Measurement of mitochondrial membrane potential

The mitochondrial membrane potential (MMP) was measured using the JC-1 fluorescent probe (Beyotime). In brief, cells were plated at a density of 3 × 10^5/well in six-well plates and exposed to apigenin for 12 h. Cells were then incubated with JC-1 for 20 min at 37°C. MMPs were determined by fluorescence microscopy and flow cytometry.

Caspase 3 activity assay

In brief, cells were incubated with apigenin for 24 h in six-well plates. The medium was replaced, and the DEVD green fluorescence probe from the Caspase 3 activity kit was added at a ratio of 1:1000. Cells were incubated with DEVD at 37°C for 30 min and harvested for further flow cytometry and fluorescence microscopy. Images were taken and merged using ImageJ software.

Transmission electron microscopy

Changes in cell ultrastructure caused by apigenin were visualized using transmission electron microscopy (TEM). The treated cells were fixed in 2.5% glutaraldehyde and post-fixed with 1% osmium tetroxide. After being dehydrated in increasing concentrations of alcohol, the cell pellets were embedded in epoxy. Representative areas were subjected to ultrathin sectioning and examined by transmission electron microscopy at × 10,000 magnification. Apoptosis was assessed by observation of nuclear chromatin condensation and edge accumulation.

Western blot analysis

Sw1353 cells (3 × 10^5) were seeded in six-well plates and treated with various concentrations of apigenin for 48 h. Cells were harvested by trypsinisation for protein extraction. Cells were resuspended in RIPA lysis buffer containing protease inhibitor cocktail (Sigma-Aldrich) for 30 min on ice and shocked every 10 min. Cell lysates were centrifuged at 13000 g for 10 min and the supernatant was collected. A BCA protein assay kit (Beyotime Institute Biotechnology) was used to quantify the protein content. Equal amounts of protein (40 μg/30 μl) were separated by 8-12% SDS-PAGE for 1.5 h at 80-120 V. The proteins were then transferred onto PVDF membranes (Millipore, Billerica, MA, USA)

at 250 mA for 2 h. The membranes were blocked with TBST containing 5% w/v bovine serum albumin (BSA, Sigma-Aldrich) for 1 h at RT and then exposed to primary antibodies at 4°C overnight. Protein bands were detected using the ChemiDoc imaging system (Bio-Rad, USA) after incubation with HRP-linked secondary antibodies for 1 h at RT. Band intensities were assessed using ImageJ software.

Human chondrosarcoma xenograft

Four-week-old female nude mice were maintained under specific pathogen-free conditions and supplied with sterilised food and water (Shanghai Laboratory Animal Center of Chinese Academy of Sciences). Sw1353 cells (5×10^6) were trypsin-digested and resuspended in 200 µl PBS, then inoculated subcutaneously into the right flank of each mouse. The tumor volume reached 200 mm^3 at 25 days after tumor cell injection. Mice were randomly divided into three groups (vehicle control, intraperitoneal injection of 2 or 5 mg/kg apigenin daily, five mice per group). Tumor size was measured and mice were weighed every 2 days. The approximate tumor volume was calculated using the formula $V = A \times B^2/2$, where A is the maximum tumor diameter and B is the minimum diameter. Apigenin treatment was continued for 2 weeks until the largest tumor reached ~1600 mm^3, and all mice were euthanised and the tumors harvested. Tumors were fixed in formalin for further analysis.

Tumor histology and immunohistochemistry

Tumor samples were subjected to hematoxylin and eosin (H&E) staining and immunohistochemical staining for Ki-67 after being formalin-fixed, sliced, dehydrated, paraffin-embedded and dewaxed. Sections (3 µm) were stained with hematoxylin for 15 min, immersed in 1% hydrochloric acid in 75% ethanol for 30 s and then in eosin for 5 min. The prepared sections were initially incubated with an anti-Ki-67 antibody at RT for 3 h and then incubated with the secondary antibody at RT for 1 h. DAB was used for colour development. Finally, the sections were immersed in xylene and mounted. Images were obtained using a DP70 CCD camera coupled to an AX-70 microscope (Olympus).

TUNEL assay

Terminal deoxynucleotidyl transferase-mediated dUTP nick-end labelling (TUNEL) assay was used to evaluate the apoptosis of xenograft tumor tissues using an In Situ Cell Death Detection Kit (Roche Diagnostics, Mannheim, Germany). In brief, after being formalin-fixed, sliced, dehydrated, paraffin-embedded, dewaxed, and incubated with proteinase K (20 µg/ml) for 25 min at 37°C, sections were incubated with fresh TUNEL reaction mixture that had been prepared for 1 h at 37°C in a humidity chamber. They were then stained with DAPI for 5 min and visualized by fluorescence microscopy. Images were merged using ImageJ software.

Statistical analysis

Data are expressed as the means ± SDs of experiments that were performed at least three times. One-way analysis of variance (ANOVA) together with Dunnett's test or an unpaired Student's t-test was used for statistical analysis. All statistical analyses were performed using SPSS software (ver. 16.0; SPSS, Inc., Chicago, IL, USA). *p*-values were two-tailed, and a p-value < 0.05 was considered to indicate statistical significance.

All procedures involving clinical specimens were approved by the Research Ethics Committee of the Second Affiliated Hospital of Zhejiang University School of Medicine, China.

Results

Apigenin inhibits proliferation of sw1353 chondrosarcoma cells

To investigate the inhibitory effect of apigenin on growth, sw1353 cells were treated with various concentrations of apigenin for 24 or 48 h. MTS assays were performed to determine the cytotoxicity of apigenin to sw1353 cells (**Figure 1B**). Cells were incubated with 100 µM apigenin, and their viability over time was determined (**Figure 1C**). A clone formation assay showed that fewer and smaller colonies formed after apigenin treatment (**Figure 1D**). These results show that apigenin inhibits the proliferation of chondrosarcoma cells in a dose- and time-dependent manner.

Apigenin induces G2/M phase arrest in sw1353 cells

To determine whether apigenin inhibits cell proliferation by inducing cell cycle arrest, we used PI staining and flow cytometry to assess the cell cycle distribution in cells treated with api-

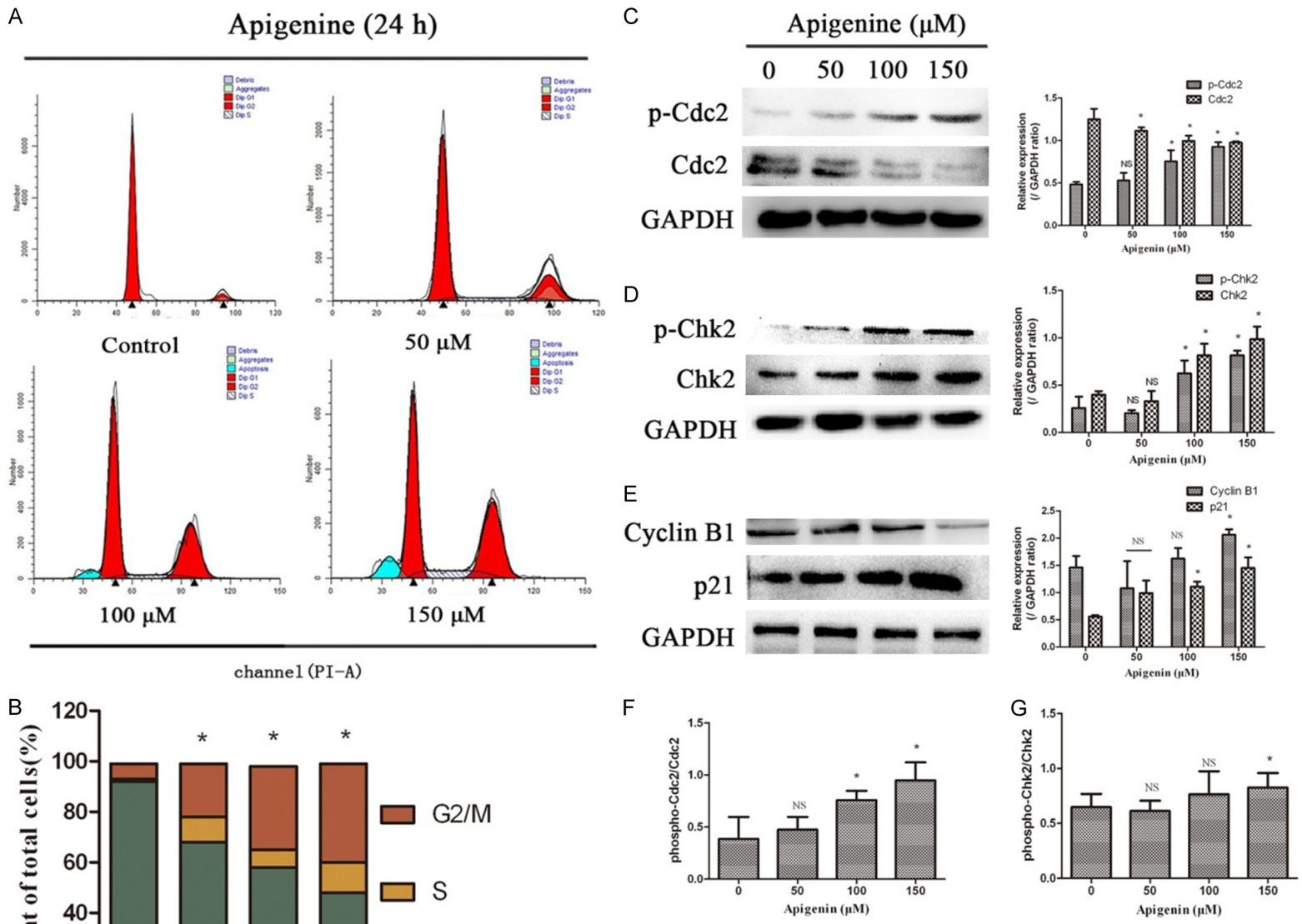

Figure 2. Apigenin induced G2/M cell cycle arrest and alters the expression of G2/M phase-related regulatory proteins in sw1353 cells. A, B. Apigenin induced G2/M phase arrest. Cells were treated with control or apigenin for 24 h and then subjected to flow cytometry. Cell cycle distribution is presented as the mean ± S.D of three independent experiments. C-G. Cells were treated with apigenin for 24 h. The expression levels of cell cycle-regulated proteins were measured by Western blotting. Band intensities were quantitatively analysed using ImageJ software, and the relative expression levels of cell cycle regulatory proteins are presented. $^{*}P < 0.05$, significantly different compared with the control. NS, not significantly different.

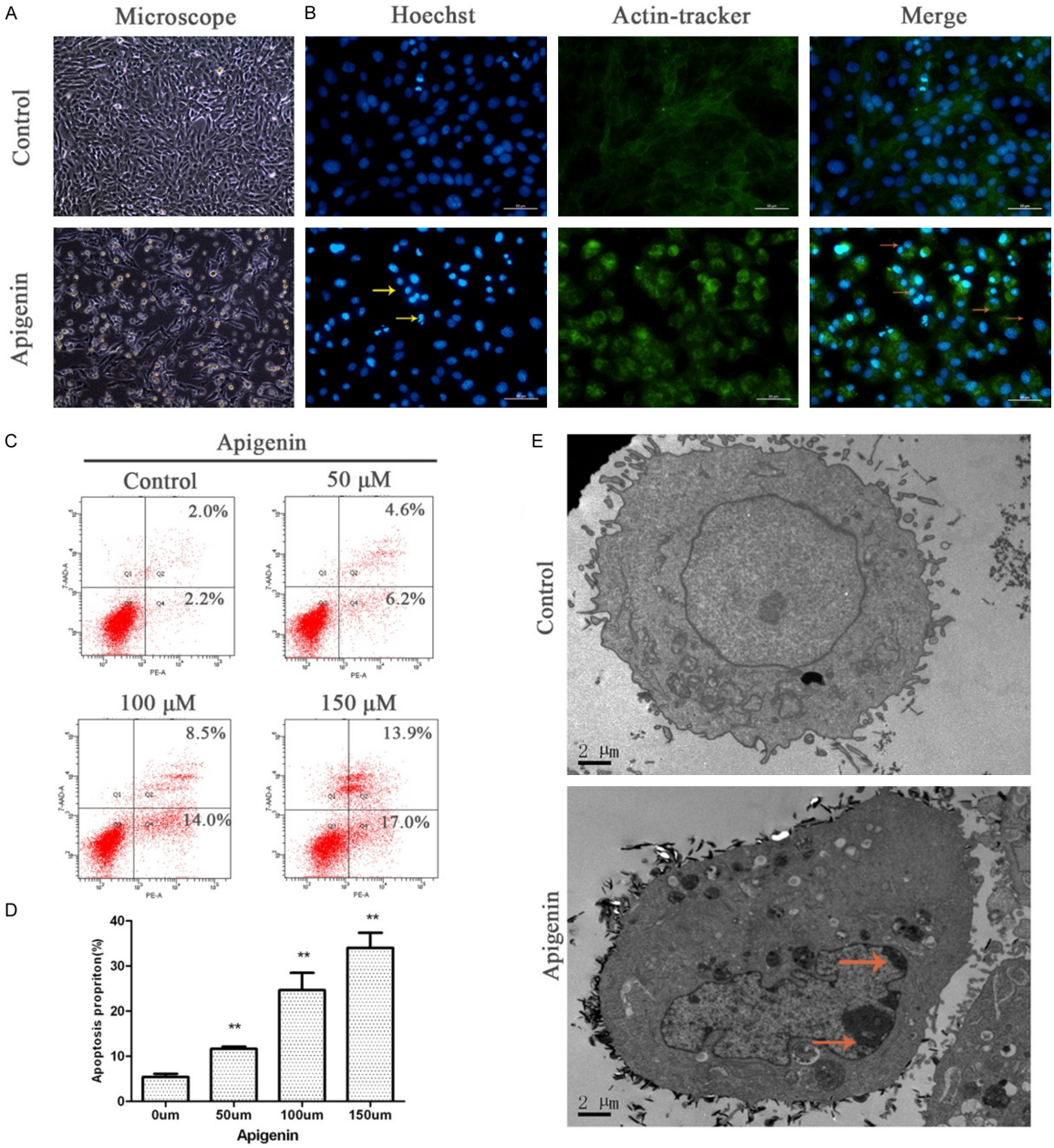

Figure 3. Apigenin induced apoptosis in sw1353 cells. A. Typical morphological changes in sw1353 cells were observed after apigenin treatment (200 × magnification). B. Hoechst 33258 and actin-tracker green staining were performed to assess cell morphology and karyopyknosis by fluorescence microscopy. Arrows indicate chromatin condensation and DNA fragmentation. Edge accumulation was observed in merged Hoechst- and actin-tracker green-stained images; bar: 50 μm. C. Cells treated with apigenin were stained with Annexin V-PE/7-AAD and analyzed by flow cytometry. Proportions of apoptotic cells from three independent experiments are shown. D. Early and late apoptosis rates as determined by flow cytometry. E. Transmission electron microscopy was used to visualize changes in nuclear ultrastructure. Arrows indicate chromatin condensation and edge accumulation. Bar: 2 μm.

genin for 24 h. Exposure to apigenin caused significant increases in the percentages of sw1353 cells in the G2/M phase (**Figure 2A**, **2B**), from 6.29% to 39%. To elucidate the mechanisms underlying cell cycle arrest, Western blotting was performed to measure the expression of cell cycle-related regulatory proteins. Apigenin upregulated the expression levels of p-Cdc2, Chk2, p-Chk2, and p21 and downregulated those of cyclin B1 and Cdc2 (**Figure 2C-G**).

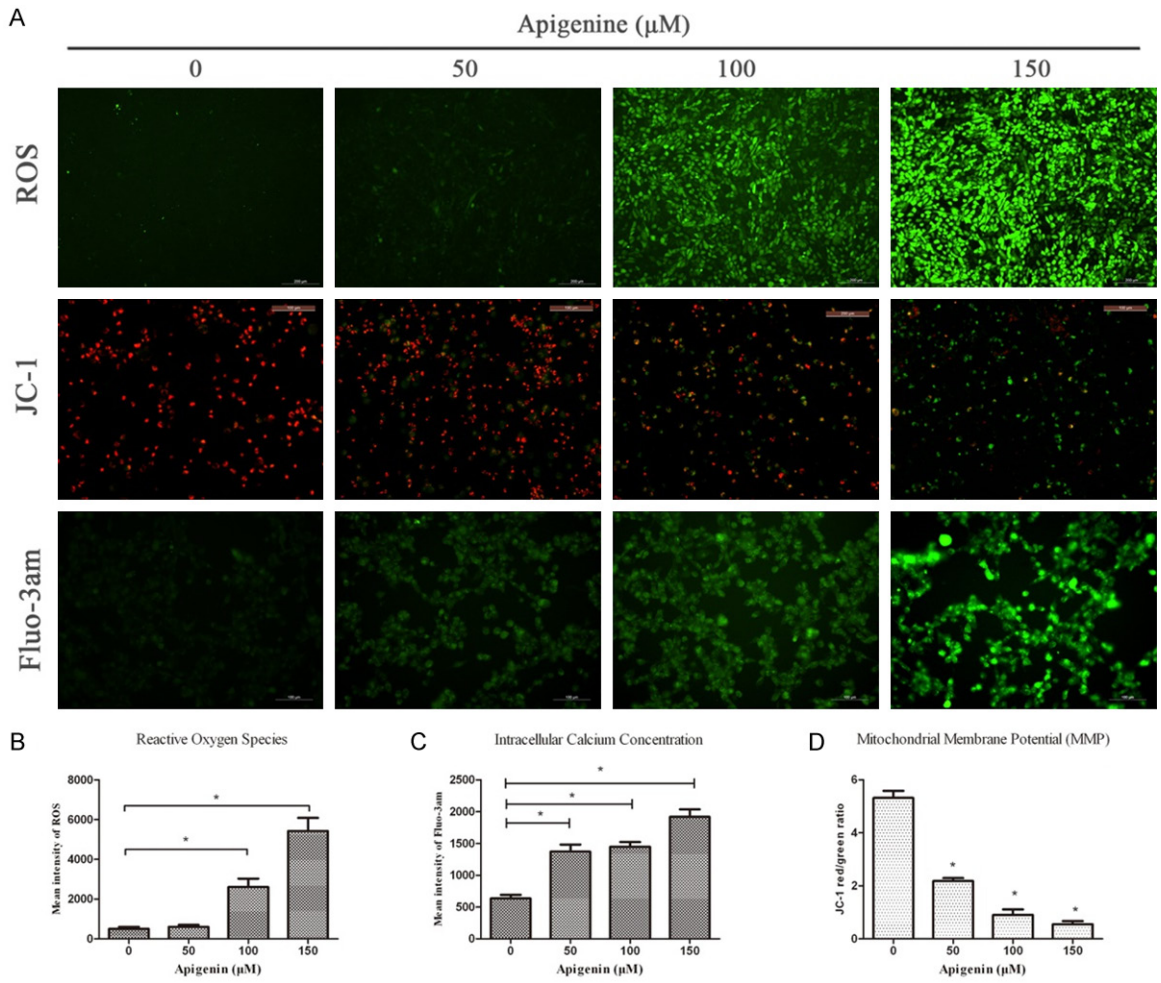

Figure 4. Apigenin induced ROS generation in sw1353 cells, which contributed to apoptosis through activation of the mitochondrial pathway. The intracellular calcium concentration increased following the suppression of mitochondrial function induced by apigenin treatment. A. Cells were treated with apigenin for 12 h and then loaded with DCFH-DA for 30 min. ROS levels were determined by fluorescence microscopy (× 200) and flow cytometry. Bar: 200 μm. MMP was measured using the JC-1 fluorescent probe and fluorescence microscopy. Changes in the JC-1 red/green ratio from three independent experiments are shown. The MMP decreased after apigenin treatment. Bar: 100 μm. The intracellular calcium concentration was measured using the fluo-3am fluorescent probe. A significant dose-dependent increase in intracellular calcium concentration was detected by fluorescence microscopy. Bar: 100 μm. B. Increase in ROS level as determined by flow cytometry and quantitative analysis. C. Increase in intracellular calcium concentration as determined by flow cytometry. D. The reduction in MMP determined by flow cytometry. Quantitative analysis of the JC-1 red/green ratio induced by the decrease in MMP. $^{*}P < 0.05$ compared with the control.

These data suggest that apigenin causes G2/M phase arrest by regulating cell cycle regulators in sw1353 cells.

Apigenin induces apoptosis in sw1353 cells

The cell morphology was observed by optical microscope (**Figure 3A**). To further investigate whether the joint action of apoptosis and cycle arrest is responsible for the inhibition of proliferation induced by apigenin, classical Hoechst 33258 staining (blue) was performed. Actin-tracker green stain (phalloidin, green, Beyotime) was used to show the shape of cells (**Figure 3B**). Hoechst staining indicated apigenin-induced apoptotic chromatin condensation and DNA fragmentation. Actin-tracker staining showed that, compared with the control group, apigenin-treated sw1353 cells exhibited shrinkage and loss of normal morphology. Edge accumulation was observed in merged Hoechst and actin-tracker green images. To quantitatively analyze apoptosis, cells were stained with annexin V-PE/7-AAD and subjected to flow cytom-

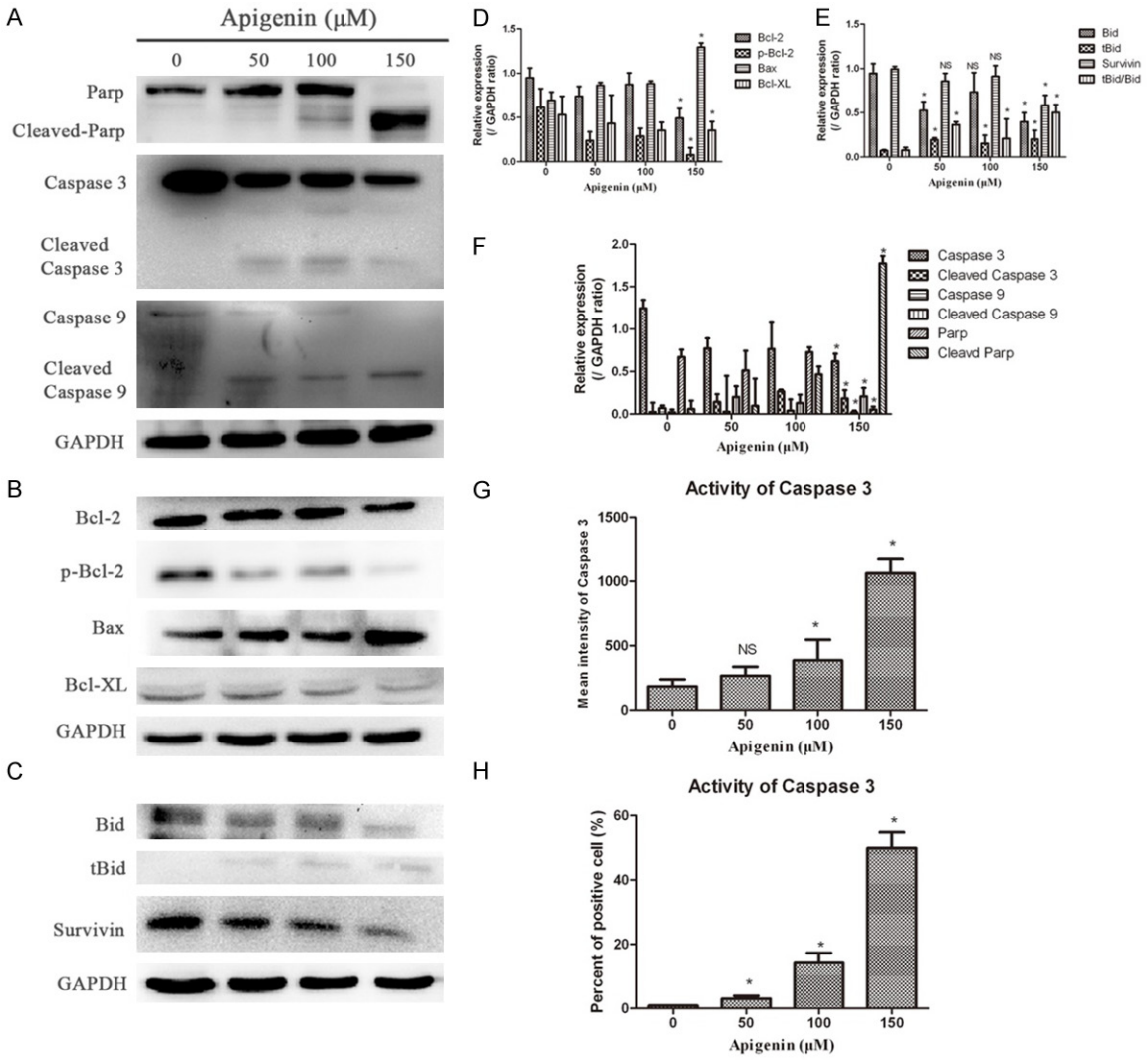

Figure 5. Apigenin altered the expression of mitochondrial apoptotic proteins in sw1353 cells. Sw1353 cells were treated with various concentrations of apigenin for 24 h. Cells were harvested and levels of apoptotic-associated Bcl-2 family and caspase cascade proteins were measured by Western blot. A, F. Parp, cleaved Parp, Caspase 3/9, and cleaved Caspase 3/9 expression levels were measured by Western blotting. Bands were quantitatively analyzed using ImageJ software. B, D. The protein levels of Bcl-2, p-Bcl-2, Bax, and Bcl-XL were determined. C, E. The levels of Bid, tBid, and survivin were determined. Caspase 3 activity was measured using the DEVD fluorescent probe at 511 nm as well as with flow cytometry and fluorescence microscopy. Bar: 100 μm. G. The mean Caspase 3 staining intensity was analyzed by flow cytometry. H. DEVD-positive cells were enumerated by flow cytometry. GAPDH was used as an internal control. Data were obtained from three independent experiments and expressed as means ± S.D. $^{*}P < 0.05$ compared with the control.

etry analysis (**Figure 3C**). The proportion of apoptotic cells was negligible in the control group, whereas apigenin treatment resulted in a dose-dependent increase in both early (Q4 quadrant) and total (Q2 + Q4 quadrant) apoptotic cells (**Figure 3D**). Transmission electron microscopy (TEM) was performed to visualize cell ultrastructure; typical apoptotic morphological features were observed. Arrows indicate chromatin condensation and edge accumulation (**Figure 3E**).

Apigenin induces mitochondrial apoptosis in sw1353 cells by inducing ROS production and mitochondrial dysfunction and disruption of intracellular calcium levels

ROS have been shown to participate in the regulation of apoptosis and cell cycle arrest [13-15]. Therefore, we investigated whether generation of ROS was involved in apigenin-induced cell death. Cells were harvested after treatment with various concentrations of apigenin

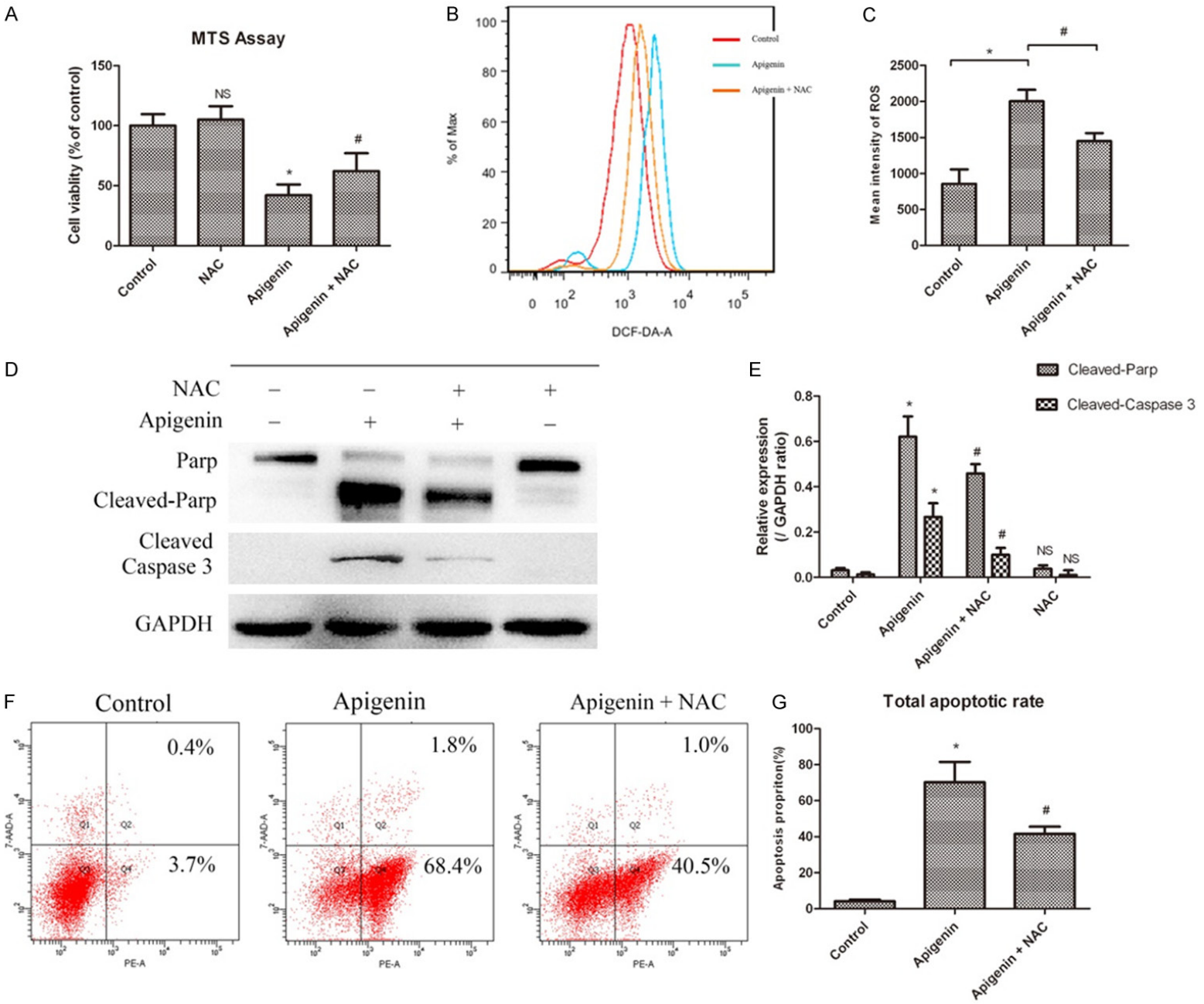
A
MTS Assay
Cell viability (% of control)
NS
*
#
Control
NAC
Apigenin
Apigenin + NAC
B
% of Max
DCF-DA-A
Control
Apigenin
Apigenin + NAC
C
Mean intensity of ROS
*
#
Control
Apigenin
Apigenin + NAC
D
NAC
Apigenin
Parp
Cleaved-Parp
Cleaved Caspase 3
GAPDH
E
Cleaved-Parp
Cleaved-Caspase 3
Relative expression (/ GAPDH ratio)
NS
Control
Apigenin
Apigenin + NAC
NAC
F
Control
Apigenin
Apigenin + NAC
0.4%
3.7%
1.8%
68.4%
1.0%
40.5%
7-AAD-A
PE-A
G
Total apoptotic rate
Apoptosis propriton(%)
Control
Apigenin
Apigenin + NAC

Figure 6. Apoptosis induced by ROS generation was blocked by the antioxidant N-acetyl-L-cysteine (NAC). Sw1353 cells were pre-incubated with NAC (5 mM) for 2 h and then treated with apigenin (150 μM) for 24 h. A. Cell viability was measured by MTS assay. B, C. ROS levels were determined by flow cytometry. Mean ROS intensities are presented as histograms. D, E. Cleaved-Parp and cleaved-Caspase 3 expression levels were measured by Western blotting. Bands were analyzed using ImageJ software. F, G. Induction of apoptosis was assessed by flow cytometry. Quantitative analysis of the total apoptotic rate. Data are means ± S.D of three independent experiments. $^{*}P < 0.05$ compared with the control; $^{\#}P < 0.05$ compared with apigenin treatment; NS, no significant difference.

for 24 h. ROS levels were measured by flow cytometry and visualized by fluorescence microscopy and staining with the fluorescent probe, DCFH-DA (Beyotime, Biotechnology). The results are shown in **Figure 4A**. ROS generation increased significantly in a dose-dependent manner. Relative fluorescence intensity in the 150-μM apigenin-treated group was 9.43-fold higher than that in the control group (**Figure 4B**). MMP decreased sharply following apigenin treatment (**Figure 4A**), which is indicative of mitochondrial dysfunction. A decrease in MMP is a sign of early apoptosis; this is usually caused by the opening of the mitochondrial permeability transition pore (MPTP), which increases the intracellular calcium ion concentration. Using JC-1, a fluorescent MMP probe, the red/green signal ratio reflects the level of apoptosis. The red staining was reduced significantly, whereas green staining was increased markedly (**Figure 4C**). Intracellular Ca^{2+} was quantified by flow cytometry and fluorescence microscopy. An increased intracellular Ca^{2+} level induces apoptosis through the endoplasmic reticulum pathway [16]. Apigenin increased the intracellular Ca^{2+} level in sw1353 cells (**Figure 4A**, **4D**). These results indicate that apigenin induces mitochondrion mediated apoptosis.

Apigenin induces apoptosis by regulating the expression of Bcl-2 family proteins and caspase cascade activation

To determine the underlying mechanism by which apigenin induces apoptosis of human chondrosarcoma cells, a Western blot analysis of the regulatory proteins in the signaling pathways involved was performed. Apigenin treatment significantly increased the expression of cleaved Caspase 3, cleaved Caspase 9, and cleaved Parp in sw1353 cells in a dose-dependent manner (**Figure 5A**, **5F**). Moreover, apigenin increased the levels of the pro-caspase protein Bax, but reduced those of the anti-apoptotic proteins Bcl-2, phospho-Bcl-2, survivin, and Bcl-XL. The levels of Bid, a pro-apoptosis protein, were decreased, possibly because of an increase in the level of its cleaved fragment, tBid (**Figure 5B-E**). Next, we assessed the activity of the effector caspase, Caspase 3, using a Cell Meter Caspase 3/7 Activity Apoptosis Assay Kit (DEVD green fluorescence), by flow cytometry (**Figure 5G**, **5H**). DEVE-positive cells were considered apoptotic. Not only the percent of caspase3-postive-cells (**Figure 5H**) but also the total mean intensity (**Figure 5G**) increased. The results suggest that apigenin induces apoptosis by regulating Bcl-2 family proteins and activating the caspase cascade in chondrosarcoma cells.

The apoptotic effect of apigenin was blocked by the antioxidant NAC in sw1353 cells

To confirm that ROS generation triggers apoptosis in sw1353 cells, the antioxidant NAC was used. Cell viability was determined by MTS assay. NAC increased the viability of apigenin-treated cells (**Figure 6A**). NAC blocked the increased ROS level induced by apigenin (**Figure 6B**, **6C**). Levels of the crucial apoptotic proteins, cleaved Parp and cleaved Caspase 3, were determined by Western blot analysis. NAC inhibited the apigenin-induced activation of apoptosis-related proteins (**Figure 6D**, **6E**). The rate of apoptosis was assessed by Annexin V and 7-AAD staining, followed by flow cytometry (**Figure 6F**, **6G**). Apigenin decreased the total apoptosis rate from 68.4% to 40.5%. These results indicate that the apoptotic effect of apigenin could be blocked by NAC, suggesting that ROS likely acts as an initiator of apigenin-induced apoptosis.

Apigenin inhibits growth of human chondrosarcoma xenografts in vivo

The *in vivo* effect of apigenin on chondrosarcoma was determined via intraperitoneal injection in a chondrosarcoma xenograft mouse model. Sw1353 cells were inoculated subcutaneously in the right flank of 4-week-old female nude mice. Intraperitoneal administration of vehicle or apigenin (2 or 5 mg/kg) daily was

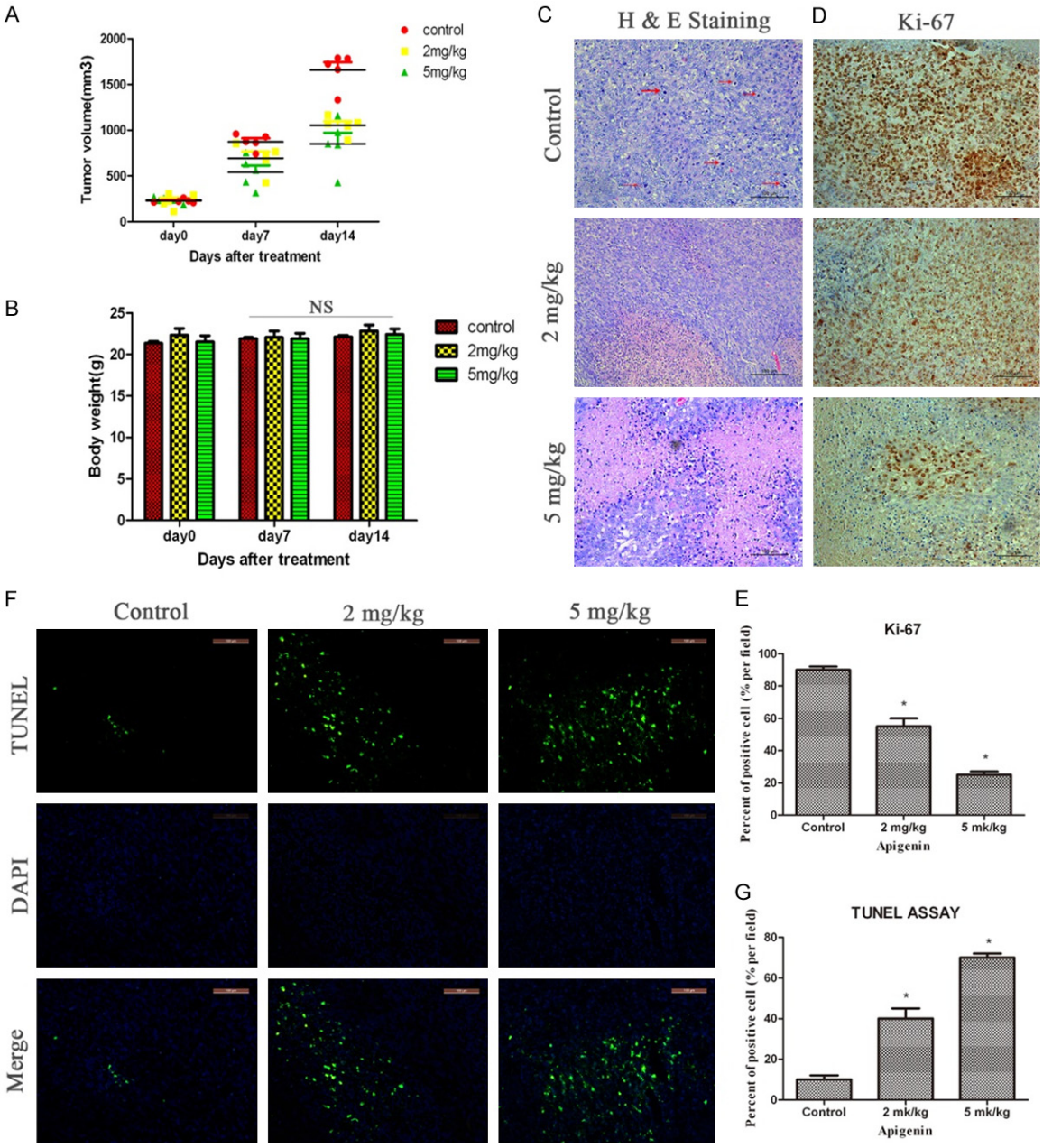

Figure 7. Apigenin inhibited growth of human chondrosarcoma xenografts in vivo. Sw1353 cells were inoculated subcutaneously into the right flank of 4-week-old female nude mice. Daily intraperitoneal administration of vehicle or apigenin (2 or 5 mg/kg) was started when tumor volume reached ~200 mm^3. All mice were euthanised at day 14. A, B. Tumor sizes and body weights were measured daily. C. H&E staining was used to evaluate histology. D, E. Immunohistochemical staining for Ki-67. F, G. The apoptotic status of tumor tissues was assessed by TUNEL assay. Representative images are presented. Bar: 100 μm. Body weight did not differ significantly between the treatment and control groups. Ki-67 and TUNEL assay data were quantitative analyzed using the IPP software. Data are expressed as means ± S.D of three independent experiments. $^*P < 0.05$ compared with the control group.

started when tumor volume reached ~200 mm^3. All mice were euthanized at day 14. The data in **Figure 7A**, **7B** reveal that intraperitoneal injection of apigenin at 2 and 5 mg/kg resulted in significant reductions in tumor volume, by 36.47% and 48.65%, respectively, after 14 days, without significant loss of body weight. H &E staining was used to perform a histological evaluation. The typical double- or multi-nucleus chondrosarcoma cells and visible myxoid degeneration were observed (**Figure 7C**). The Ki-67 protein (also known as MKI67) is a cellular

marker of proliferation [17]. Immunohistochemical staining showed that apigenin treatment inhibited the expression of Ki-67 (**Figure 7D**, **7E**). TUNEL assay indicated evident increasing apoptosis cells (**Figure 7F**, **7G**). These results reveal that apigenin inhibits the growth of chondrosarcoma cells *in vivo* with little toxicity.

Discussion

Chondrosarcoma is a malignant tumor that produces cartilage matrix. Chondrosarcomas account for up to 27% of all primary malignant bone tumors, second only to osteosarcoma in adults [18]. Due to its marked resistance to conventional chemo- and radiotherapy, wide-margin surgical resection remains the only curative treatment for this tumor. Therefore, the prognosis is poor for unresectable and metastatic disease [19-21]. A novel adjuvant therapy for chondrosarcoma is thus required.

Apigenin inhibits the growth of cancer cells, including head-and-neck squamous cell carcinoma, hepatoma, and bladder cancer cells [22-25], and plays an important adjuvant role in therapy with other agents [22, 26]. The current study examined the anti-neoplastic effect of apigenin on chondrosarcoma cells *in vitro* and *in vivo*. Our results indicate that apigenin inhibits the proliferation of human chondrosarcoma cells by inducing G2/M arrest and mitochondrial apoptosis, an effect mediated by ROS generation.

Cell cycle arrest is regulated by cell cycle checkpoints after DNA damage. DNA damage triggers the activation of the kinase ataxia telangiectasia mutated (ATM)/ataxia telangiectasia- and Rad3-related (ATR) pathway, in which ATM/ATR phosphorylate and activate the Chk1/Chk2 checkpoint kinases. The expression of Chk2 and its phosphorylation activates the p53-p21 pathway, p21 being an inhibitor of the cyclins/CDKs that regulate cell cycle arrest [27, 28]. The cyclin B1/Cdc2 complex, which is kept inactive by the phosphorylation of Cdc2 (CDK1), plays a key role in promoting the G2/M phase transition [29]. Our study demonstrated that apigenin induced G2/M arrest by upregulating the rates of p-Cdc2/Cdc2 and P-Chk2/Chk2 and the expression of p21, while downregulating cyclin B1. Cyclin B1 expression is increased during G2/M cell cycle arrest [30-32]. Li recently reported that G2/M arrest in osteosarcoma cells treated with celastrol was associated with increased expression of Cyclin B1 [30-32]. However, Zhang suggested that cyclin B1 expression was downregulated in cells with piperine-induced G2/M arrest [33]. It is possible that downregulation of Cdc2 activity suppresses ubiquitin-dependent Cyclin B1 degradation, which leads to an increase in Cyclin B1 levels [31, 32]. In our opinion, levels of cyclin B1 oscillate over the course of the cell cycle. Cyclin B1 accumulates throughout the cell cycle and is activated by Cdc2 at the beginning of G2 phase. It is degraded at the end of mitosis (M phase). Thus, its expression changes at different time points during the G2/M phase. The expression of Cyclin B1 is increased by arrest at the G2 phase. By contrast, Cyclin B1 expression decreases when cells are arrested in late M phase. It was reported that apigenin causes G1/G0 phase arrest in prostate cancer cells [6, 34]. Iizumi reported that apigenin induces G2/M arrest at least in part by directly binding and inhibiting ribosomal protein S9 (RPS9), which enhances CDK1 expression [35]. Our findings suggest that apigenin exerts a marked effect on the cell cycle distribution in chondrosarcoma cells.

Apoptosis, an important means of eliminating cancer cells, is divided into extrinsic (death receptor-dependent pathway) and intrinsic (mitochondria-dependent pathway) pathways [36]. Bcl-2 family (B-cell lymphoma 2) proteins play a critical role in the intrinsic pathway [12]. The intrinsic pathway (or mitochondrial pathway) involves mitochondria as the central regulator and is associated with the apoptotic regulatory factors Bcl-2 family proteins and Caspases [37, 38]. Caspases are essential for apoptosis [39, 40], and they have been termed “executioner” proteins because of their role in cells. In the current study, we assessed the expression and phosphorylation of the anti-apoptotic proteins Bcl-2 and Bcl-XL, and the pro-apoptotic proteins, Bax, Bid, and tBid. Apigenin treatment downregulated both the level and phosphorylation of Bcl-2 and Bcl-XL, upregulated Bax, and increased the tBid/Bid ratio. As expected, the downregulation of anti-apoptotic proteins and the upregulation of pro-apoptotic proteins induced by apigenin led to cytochrome C release from mitochondria and initiation of the caspase cascade [41, 42]. Cytochrome C cleaved and activated the initiator caspase, Caspase 9, which cleaved and thereby activated the effector

caspase, Caspase 3. Cleaved Parp formation is considered an indicator of Caspase 3 activation. Moreover, although caspases can cleave Bcl-2 family proteins to initiate apoptosis [43, 44], it did not do so in our experiment. The BH3-only pro-apoptotic Bcl-2 family member Bid is cleaved into truncated Bid (tBid). The cleavage of Bid is considered a conversion point from the extrinsic to intrinsic apoptosis pathways [45, 46]. Truncated Bid translocates to the mitochondria and induces loss of mitochondrial membrane potential (MMP) and the release of apoptogenic factors, including cytochrome C. Survivin, an anti-apoptotic protein, functions to inhibit caspase 3 activation, thereby leading to the negative regulation of apoptosis [47, 48]. Apigenin treatment suppressed the expression of survivin and induced apoptosis in chondrosarcoma cells.

ROS are involved in maintaining cell homeostasis and regulating cellular signal transduction under normal physiological conditions [49]. However, ROS-mediated DNA damage is considered to contribute to carcinogenesis initiation and malignant transformation [14, 50, 51]. ROS has been developed as a promising target of pharmaceutical therapy for several malignancies [32, 52, 53]. Excessive ROS may induce apoptosis through both the extrinsic and intrinsic pathways [15, 53]. In the intrinsic pathway, ROS function to stimulate cytochrome C release via activating anti-apoptotic proteins (Bcl-2 and Bcl-XL) and inhibiting pro-apoptotic proteins (Bax and Bid) [54, 55]. Using flow cytometry and fluorescent staining, we found that apigenin induced excessive ROS generation. We believe that excessive ROS generation activated the intrinsic apoptotic pathway, leading to the initiation of the caspase cascade and, finally, to apoptosis in chondrosarcoma cells. The ROS-mediated oxidative damage resulted in a decline in mitochondrial function [14, 49]. The JC-1 fluorescent probe was used to assess the MMP. The MMP in sw1353 cells decreased significantly after incubation with apigenin. The decrease in mitochondrial function led to an imbalance in intracellular calcium ion concentration. The probe fluo-3am was used to evaluate intracellular calcium accumulation. Apoptosis is usually accompanied by an increase in the intracellular calcium concentration. Shi et al. demonstrated that apigenin inhibited proliferation of human bladder cancer cells via cell cycle arrest and apoptosis induced by ROS generation [24]. Zhang et al. reported that apigenin induces autophagic death in human papillary thyroid carcinoma cells via enhancing ROS generation [56]. These findings are in agreement with our finding that apigenin accelerates ROS generation and promotes apoptosis in certain malignancies.

Treatment of chondrosarcoma tumor-bearing nude mice with 2 and 5 mg/kg apigenin resulted in significant inhibition of tumor growth (36-48%) without loss of body weight according to our in vivo experiment. No gross toxicity was detected. The typical double- or multi-nucleus chondrosarcoma cells and visible myxoid degeneration were observed by H&E staining. The numerous Ki-67-positive nuclei in the control group indicated exuberant tumor cell growth. These results demonstrated that sw1353 cells are a high-grade malignancy. Apigenin treatment resulted in the death of numerous tumor cells (**Figure 6C**, treatment group), and TUNEL assay confirmed the apoptosis of chondrosarcoma cells (**Figure 6F**). The DAPI staining results were consistent with those of the TUNEL assay. Numerous nuclear pyknoses were found in TUNEL-positive regions (**Figure 6F**, DAPI), and the number of Ki-67–positive nuclei decreased markedly after apigenin treatment (**Figure 6D**). These in vivo results indicate that apigenin may have potential as an adjuvant therapy for chondrosarcoma.

In conclusion, to our knowledge, this is the first report that apigenin can inhibit the proliferation of chondrosarcoma cells by G2/M arrest and induction of apoptosis via ROS generation. In a chondrosarcoma xenograft model, apigenin markedly suppressed tumor growth without causing toxicity. These findings suggest apigenin is a promising adjuvant therapy for chondrosarcoma.

Disclosure of conflict of interest

None.

Address correspondence to: Zhao-Ming Ye, Department of Orthopedics, Second Affiliated Hospital, School of Medicine, Zhejiang University, No.88 Jiefang Road, Hangzhou 310009, Zhejiang, PR. China. Tel: +86 571 89713641; Fax: +86 571 87783688; E-mail: 2192002@zju.edu.cn

References

[1] Papachristou DJ and Papavassiliou AG. Osteosarcoma and chondrosarcoma: new signaling pathways as targets for novel therapeutic interventions. Int J Biochem Cell Biol 2007; 39: 857-862.

[2] Van Gompel JJ and Janus JR. Chordoma and chondrosarcoma. Otolaryngol Clin North Am 2015; 48: 501-514.

[3] Terek RM. Recent advances in the basic science of chondrosarcoma. Orthop Clin North Am 2006; 37: 9-14.

[4] Sonne-Holm E, Wong C and Sonne-Holm S. Multiple cartilaginous exostoses and development of chondrosarcomas–a systematic review. Dan Med J 2014; 61: A4895.

[5] Leddy LR and Holmes RE. Chondrosarcoma of bone. Cancer Treat Res 2014; 162: 117-130.

[6] Shukla S, Fu P and Gupta S. Apigenin induces apoptosis by targeting inhibitor of apoptosis proteins and Ku70-Bax interaction in prostate cancer. Apoptosis 2014; 19: 883-894.

[7] Seo HS, Jo JK, Ku JM, Choi HS, Choi YK, Woo JK, Kim HI, Kang SY, Lee KM, Nam KW, Park N, Jang BH, Shin YC and Ko SG. Induction of caspase-dependent extrinsic apoptosis by apigenin through inhibition of signal transducer and activator of transcription 3 (STAT3) signalling in HER2-overexpressing BT-474 breast cancer cells. Biosci Rep 2015; 35.

[8] Zeng P, Liu B, Wang Q, Fan Q, Diao JX, Tang J, Fu XQ and Sun XG. Apigenin attenuates atherogenesis through inducing macrophage apoptosis via Inhibition of AKT Ser473 phosphorylation and downregulation of plasminogen activator inhibitor-2. Oxid Med Cell Longev 2015; 2015: 379538.

[9] Chen C, He H, Luo Y, Zhou M, Yin D and He M. Involvement of Bcl-2 signal pathway in the protective effects of apigenin on anoxia/reoxygenation-induced myocardium injury. J Cardiovasc Pharmacol 2016; 67: 152-163.

[10] Shukla S and Gupta S. Apigenin-induced prostate cancer cell death is initiated by reactive oxygen species and p53 activation. Free Radic Biol Med 2008; 44: 1833-1845.

[11] Fonseca-Silva F, Canto-Cavalheiro MM, Menna-Barreto RF and Almeida-Amaral EE. Effect of apigenin on leishmania amazonensis is associated with reactive oxygen species production followed by mitochondrial dysfunction. J Nat Prod 2015; 78: 880-884.

[12] Hengartner MO. The biochemistry of apoptosis. Nature 2000; 407: 770-776.

[13] Simon HU, Haj-Yehia A and Levi-Schaffer F. Role of reactive oxygen species (ROS) in apoptosis induction. Apoptosis 2000; 5: 415-418.

[14] Fruehauf JP and Meyskens FL Jr. Reactive oxygen species: a breath of life or death? Clin Cancer Res 2007; 13: 789-794.

[15] Ozben T. Oxidative stress and apoptosis: impact on cancer therapy. J Pharm Sci 2007; 96: 2181-2196.

[16] Zou P, Xia Y, Chen T, Zhang J, Wang Z, Chen W, Chen M, Kanchana K, Yang S and Liang G. Selective killing of gastric cancer cells by a small molecule targeting ROS-mediated ER stress activation. Mol Carcinog 2016; 55: 1073-1086.

[17] Scholzen T and Gerdes J. The Ki-67 protein: from the known and the unknown. J Cell Physiol 2000; 182: 311-322.

[18] Gelderblom H, Hogendoorn PC, Dijkstra SD, van Rijswijk CS, Krol AD, Taminiau AH and Bovee JV. The clinical approach towards chondrosarcoma. Oncologist 2008; 13: 320-329.

[19] Lee FY, Mankin HJ, Fondren G, Gebhardt MC, Springfield DS, Rosenberg AE and Jennings LC. Chondrosarcoma of bone: an assessment of outcome. J Bone Joint Surg Am 1999; 81: 326-338.

[20] Bovee JV, Cleton-Jansen AM, Taminiau AH and Hogendoorn PC. Emerging pathways in the development of chondrosarcoma of bone and implications for targeted treatment. Lancet Oncol 2005; 6: 599-607.

[21] Bauer HC, Brosjo O, Kreicbergs A and Lindholm J. Low risk of recurrence of enchondroma and low-grade chondrosarcoma in extremities. 80 patients followed for 2-25 years. Acta Orthop Scand 1995; 66: 283-288.

[22] Chan LP, Chou TH, Ding HY, Chen PR, Chiang FY, Kuo PL and Liang CH. Apigenin induces apoptosis via tumor necrosis factor receptor- and Bcl-2-mediated pathway and enhances susceptibility of head and neck squamous cell carcinoma to 5-fluorouracil and cisplatin. Biochim Biophys Acta 2012; 1820: 1081-1091.

[23] Cai J, Zhao XL, Liu AW, Nian H and Zhang SH. Apigenin inhibits hepatoma cell growth through alteration of gene expression patterns. Phytomedicine 2011; 18: 366-373.

[24] Shi MD, Shiao CK, Lee YC and Shih YW. Apigenin, a dietary flavonoid, inhibits proliferation of human bladder cancer T-24 cells via blocking cell cycle progression and inducing apoptosis. Cancer Cell Int 2015; 15: 33.

[25] Zhang Q, Cheng G, Qiu H, Zhu L, Ren Z, Zhao W, Zhang T and Liu L. The p53-inducible gene 3 involved in flavonoid-induced cytotoxicity through the reactive oxygen species-mediated mitochondrial apoptotic pathway in human hepatoma cells. Food Funct 2015; 6: 1518-1525.

[26] Yang L, Allred KF, Dykes L, Allred CD and Awika JM. Enhanced action of apigenin and naringenin combination on estrogen receptor activation in non-malignant colonocytes: implications on sorghum-derived phytoestrogens. Food Funct 2015; 6: 749-755.

[27] Weinert T and Lydall D. Cell cycle checkpoints, genetic instability and cancer. Semin Cancer Biol 1993; 4: 129-140.
[28] Kastan MB and Bartek J. Cell-cycle checkpoints and cancer. Nature 2004; 432: 316-323.
[29] Nurse P. Universal control mechanism regulating onset of M-phase. Nature 1990; 344: 503-508.
[30] Knowles LM and Milner JA. Diallyl disulfide inhibits p34 (cdc2) kinase activity through changes in complex formation and phosphorylation. Carcinogenesis 2000; 21: 1129-1134.
[31] Lin H, Liu XY, Subramanian B, Nakeff A, Valeriote F and Chen BD. Mitotic arrest induced by XK469, a novel antitumor agent, is correlated with the inhibition of cyclin B1 ubiquitination. Int J Cancer 2002; 97: 121-128.
[32] Li HY, Zhang J, Sun LL, Li BH, Gao HL, Xie T, Zhang N and Ye ZM. Celastrol induces apoptosis and autophagy via the ROS/JNK signaling pathway in human osteosarcoma cells: an in vitro and in vivo study. Cell Death Dis 2015; 6: e1604.
[33] Zhang J, Zhu X, Li H, Li B, Sun L, Xie T, Zhu T, Zhou H and Ye Z. Piperine inhibits proliferation of human osteosarcoma cells via G2/M phase arrest and metastasis by suppressing MMP-2/-9 expression. Int Immunopharmacol 2015; 24: 50-58.
[34] Shukla S, Bhaskaran N, Babcook MA, Fu P, Maclennan GT and Gupta S. Apigenin inhibits prostate cancer progression in TRAMP mice via targeting PI3K/Akt/FoxO pathway. Carcinogenesis 2014; 35: 452-460.
[35] Iizumi Y, Oishi M, Taniguchi T, Goi W, Sowa Y and Sakai T. The flavonoid apigenin downregulates CDK1 by directly targeting ribosomal protein S9. PLoS One 2013; 8: e73219.
[36] Thornberry NA, Rano TA, Peterson EP, Rasper DM, Timkey T, Garcia-Calvo M, Houtzager VM, Nordstrom PA, Roy S, Vaillancourt JP, Chapman KT and Nicholson DW. A combinatorial approach defines specificities of members of the caspase family and granzyme B. Functional relationships established for key mediators of apoptosis. J Biol Chem 1997; 272: 17907-17911.
[37] Czabotar PE, Westphal D, Dewson G, Ma S, Hockings C, Fairlie WD, Lee EF, Yao S, Robin AY, Smith BJ, Huang DC, Kluck RM, Adams JM and Colman PM. Bax crystal structures reveal how BH3 domains activate Bax and nucleate its oligomerization to induce apoptosis. Cell 2013; 152: 519-531.
[38] Li T, Kon N, Jiang L, Tan M, Ludwig T, Zhao Y, Baer R and Gu W. Tumor suppression in the absence of p53-mediated cell-cycle arrest, apoptosis, and senescence. Cell 2012; 149: 1269-1283.
[39] Jin Z, Li Y, Pitti R, Lawrence D, Pham VC, Lill JR and Ashkenazi A. Cullin3-based polyubiquitination and p62-dependent aggregation of caspase-8 mediate extrinsic apoptosis signaling. Cell 2009; 137: 721-735.
[40] Ricci JE, Munoz-Pinedo C, Fitzgerald P, Bailly-Maitre B, Perkins GA, Yadava N, Scheffler IE, Ellisman MH and Green DR. Disruption of mitochondrial function during apoptosis is mediated by caspase cleavage of the p75 subunit of complex I of the electron transport chain. Cell 2004; 117: 773-786.
[41] Cipolat S, Rudka T, Hartmann D, Costa V, Serneels L, Craessaerts K, Metzger K, Frezza C, Annaert W, D'Adamio L, Derks C, Dejaegere T, Pellegrini L, D'Hooge R, Scorrano L and De Strooper B. Mitochondrial rhomboid PARL regulates cytochrome c release during apoptosis via OPA1-dependent cristae remodeling. Cell 2006; 126: 163-175.
[42] Kuida K, Haydar TF, Kuan CY, Gu Y, Taya C, Karasuyama H, Su MS, Rakic P and Flavell RA. Reduced apoptosis and cytochrome c-mediated caspase activation in mice lacking caspase 9. Cell 1998; 94: 325-337.
[43] Cheng EH, Kirsch DG, Clem RJ, Ravi R, Kastan MB, Bedi A, Ueno K and Hardwick JM. Conversion of Bcl-2 to a Bax-like death effector by caspases. Science 1997; 278: 1966-1968.
[44] Fujita N and Tsuruo T. Involvement of Bcl-2 cleavage in the acceleration of VP-16-induced U937 cell apoptosis. Biochem Biophys Res Commun 1998; 246: 484-488.
[45] Luo X, Budihardjo I, Zou H, Slaughter C and Wang X. Bid, a Bcl2 interacting protein, mediates cytochrome c release from mitochondria in response to activation of cell surface death receptors. Cell 1998; 94: 481-490.
[46] Kantari C and Walczak H. Caspase-8 and bid: caught in the act between death receptors and mitochondria. Biochim Biophys Acta 2011; 1813: 558-563.
[47] Pandey A, Vishnoi K, Mahata S, Tripathi SC, Misra SP, Misra V, Mehrotra R, Dwivedi M and Bharti AC. Berberine and curcumin target survivin and STAT3 in gastric cancer cells and synergize actions of standard chemotherapeutic 5-Fluorouracil. Nutr Cancer 2015; 67: 1293-1304.
[48] Soleimanpour E and Babaei E. Survivin as a potential target for cancer therapy. Asian Pac J Cancer Prev 2015; 16: 6187-6191.
[49] Ray PD, Huang BW and Tsuji Y. Reactive oxygen species (ROS) homeostasis and redox regulation in cellular signaling. Cell Signal 2012; 24: 981-990.
[50] Valko M, Leibfritz D, Moncol J, Cronin MT, Mazur M and Telser J. Free radicals and antioxidants in normal physiological functions and

human disease. Int J Biochem Cell Biol 2007; 39: 44-84.
[51] Voloboueva LA, Duan M, Ouyang Y, Emery JF, Stoy C and Giffard RG. Overexpression of mitochondrial Hsp70/Hsp75 protects astrocytes against ischemic injury in vitro. J Cereb Blood Flow Metab 2008; 28: 1009-1016.
[52] Wu J, Song T, Liu S, Li X, Li G and Xu J. Icariside II inhibits cell proliferation and induces cell cycle arrest through the ROS-p38-p53 signaling pathway in A375 human melanoma cells. Mol Med Rep 2015; 11: 410-416.
[53] Zhang X, Wang X, Wu T, Li B, Liu T, Wang R, Liu Q, Liu Z, Gong Y and Shao C. Isoliensinine induces apoptosis in triple-negative human breast cancer cells through ROS generation and p38 MAPK/JNK activation. Sci Rep 2015; 5: 12579.
[54] Filippova M, Filippov V, Williams VM, Zhang K, Kokoza A, Bashkirova S and Duerksen-Hughes P. Cellular levels of oxidative stress affect the response of cervical cancer cells to chemotherapeutic agents. Biomed Res Int 2014; 2014: 574659.
[55] Lopes M, Mota M and Belo I. Comparison of Yarrowia lipolytica and Pichia pastoris cellular response to different agents of oxidative stress. Appl Biochem Biotechnol 2013; 170: 448-458.
[56] Zhang L, Cheng X, Gao Y, Zheng J, Xu Q, Sun Y, Guan H, Yu H and Sun Z. Apigenin induces autophagic cell death in human papillary thyroid carcinoma BCPAP cells. Food Funct 2015; 6: 3464-3472.